Chapter 34
Latest GNSS Results of the CMONOC Network and Its Application in Earthquake Monitoring

Junping Chen, Yize Zhang, Yibing Xie, Weijie Tan, Sainan Yang and Bin Wu

Abstract Crustal Movement Observation Network Of China (CMONOC) is a fundamental facility which has wide-range applications in diverse areas with high precision and high spatial resolution. CMONOC network consists of GNSS, VLBI, SLR and gravity observing stations. The observation data contributes to the GNSS meteorology, plate tectonics and earthquake monitoring etc. Shanghai Astronomical Observatory (SHAO) is one of the data centers of the CMONOC network. We developed the CMONOC GNSS data processing platform and provide precise products supporting CMONOC applications. In this paper, we present the latest results from the routine data analysis. Besides the conventional results of GNSS orbits, clocks, ERPs and station coordinates etc., we present for the first time the following results: (1) regional velocity field for the 247 continuous stations, which is derived based on integrated data analysis of the CMONOC and IGS network; (2) earthquake monitoring by ionosphere disturbance analysis, which is realized by analyzing the ionosphere TEC changes time series using the quartile method; (3) earthquake monitoring by instantaneous station motion analysis, which is determined by differential 1 Hz phase observation in real-time.

Keywords CMONOC · GGDAA · Velocity field · Earthquake · Ionosphere

J. Chen (✉) · Y. Zhang · Y. Xie · W. Tan · S. Yang · B. Wu
Shanghai Astronomical Observatory, Chinese Academy of Science, Shanghai, People's Republic of China
e-mail: junping@shao.ac.cn

Y. Zhang · Y. Xie
College of Surveying and Geo-Informatics, Tongji University, Shanghai, People's Republic of China

34.1 Introduction

Crustal Movement Observation Network Of China (CMONOC) is in operation since 1999. It is a fundamental facility which has wide-range applications in diverse areas with high precision and high spatial resolution. It consists of 260 GNSS stations, several Very Long Baseline Radio Interferometry (VLBI) and Satellite Ranging (SLR) and precise leveling and gravity stations. Observation data of CMONOC make an important contribution in the field of research concerning the GNSS meteorology [1], plate tectonics and earthquake monitoring [2].

As one of the data center of the CMONOC, Shanghai Astronomical Observatory (SHAO) operates the routine GNSS data analysis since June 2011 [3]. Data analysis implements similar strategies as it used in our IGS routine data analysis [4]. In the CMONOC routine analysis, we combine the observations from the IGS and CMONOC network, and all solutions are aligned to the ITRF2008 frame. Figure 34.1 shows the number of stations processed in our routine job, where around 300 stations are processed per day with around 80 are IGS sites. Based on daily solutions, precise orbits, clocks, troposphere and coordinates etc. are derived [5]. Besides these precise products, we present for the first time the following new results: (1) regional velocity field for the 247 continuous stations, which is derived based on integrated data analysis of the CMONOC and IGS network; (2) earthquake monitoring by ionosphere disturbance analysis, which is realized by analyzing the ionosphere TEC changes time series using the quartile method; (3) earthquake monitoring by instantaneous station motion analysis, which is determined by differential 1 Hz phase observation in real-time.

34.2 Velocity Field of the CMONOC GNSS Stations

We start the daily solution since January 2011, which includes 252 stations till December 2013. To obtain velocity field of the continental China, we combine all the daily solutions using the software Quasi-observation Combination Analysis (QOCA, http://gipsy.jpl.nasa.gov/qoca) [6]. The strategy of data combination follows the following 3 steps: (1) generation of the daily solutions, which are under the ITRF2008 frame; (2) data combination using the package of analyze_ tseri of QOCA to get velocity of continental China for the 247 stations with data interval longer than 1 year; (3) velocity transformation from global ITRF2008 frame to the stable Eurasia plate (EURA).

In the data combination using QOCA, we carry out data editing for the time series jumps due to known events, including coseismic offsets due to the Japan earthquake in 2011 and Lushan earthquake in 2013; nonlinear variations of some stations as YNXP, YNJD and YNSM in Yunnan province. Annual/semiannual periodical motion is considered for all sites. In additional we perform the principal component analysis (PCA) to remove the common mode error from each raw time
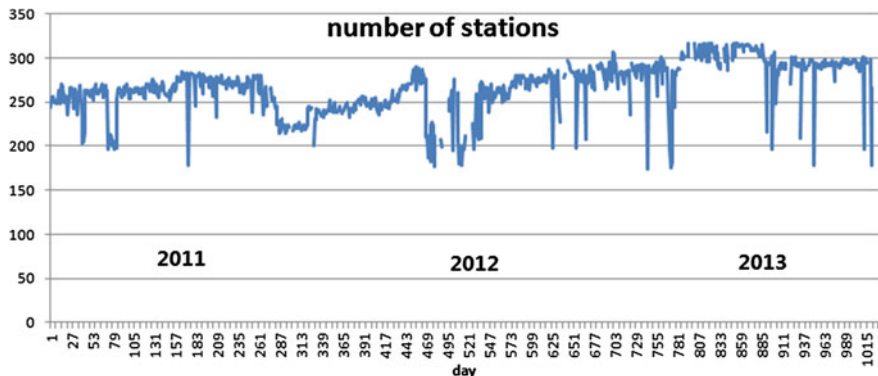
Fig. 34.1 Number of stations processed at the SHAO, where around 80 stations are from the IGS global tracking network. Data analysis is in daily batch with latency of 1 day, and stations with latency of more than 1 day in data transfer are not included in the daily solution
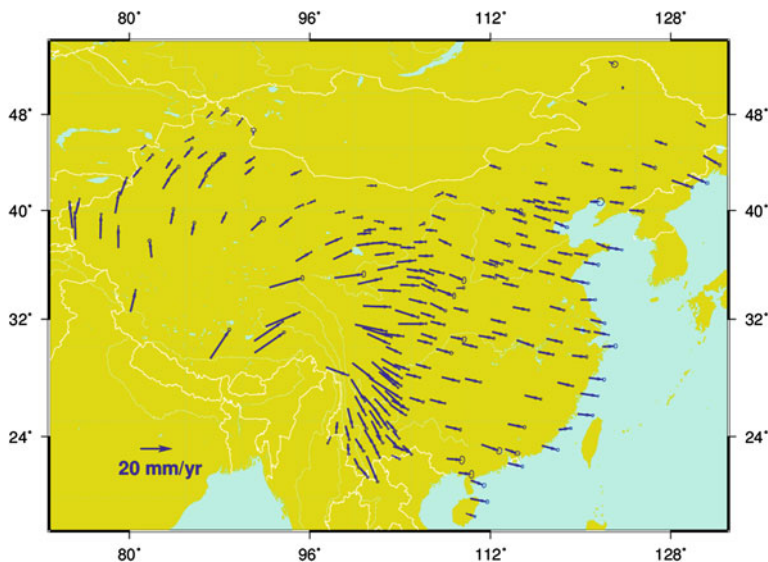

Fig. 34.2 CMONOC GPS result of the horizontal velocity field of continental China respect to EURA. The arrows represent the velocities. The ellipses represent the 95 % confidence level

series [7]. For the velocity transformation, we follow the NNR-NUVEL model and select 11 reference stations [8] to calculate the Euler vector of the EURA plate. Weighted least squares algorithm is applied in the estimation of the Euler vectors through an iterative process [9]. The resulting Euler vectors are (54.30°N, 100.30°W), and 0.253°/M.a. The horizontal velocity field of continental China respect to EURA is shown in Fig. 34.2, where 247 stations are included.

34.3 Ionospheric Disturbance Monitoring Using the CMONOC Network

Ionosphere abnormal disturbances were observed for the first time in the 1965 Alaska earthquake [10], and the analysis of the seismic ionospheric disturbances is developed since then. The comparison between the instantaneous TEC and statistical quantity of Total Electron Content (TEC) reflects such disturbances [11]. Statistical quantity of TEC could be selected according to the quartile definition, where the first quartile (designated Q1) splits off the lowest 25 % of data from the highest 75 %; and the second quartile (designated Q2) cuts data set in half; the third quartile (designated Q3) splits off the highest 25 % of data from the lowest 75 %. The difference between the Q3 and Q1 quartiles is called the interquartile range (IQR). We define in this paper the upper quartile L1 as the sum of the Q2 and IQR and the lower quartile L2 as the difference between Q2 and IQR. Ionospheric disturbances is detected when the instantaneous TEC is not within the range defined by the upper and lower quartiles.

According to [11], the TEC quartiles at current epoch is calculated using a sample of 15 TECs, where the TECs at same epoch of successive 15 days are used. We set up the ionospheric disturbances monitoring system based on this strategy and the system run in the following way: (1) calculation of the Vertical TEC (VTEC) using precise models, e.g. the Global Ionospheric Mapping (GIM) of the IGS; (2) calculation the real-time VTEC and VTEC quartiles of current epoch; (3) comparison between real-time VTEC and VTEC quartiles to check for ionospheric disturbances.

Taking the Lushan (Sichuan Province) M_S7.0 earthquake on April 20, 2013 as an example. We use the IGS GIM data to calculate the VTEC over the epicenter (30.3° N, 103.0° E), as shown in Fig. 34.3. From Fig. 34.3, VTEC disturbance is obvious on April 16–21 with observed VTEC below the VTEC lower bounds (L2), especially on the day before earthquake. The VTEC gradually return to normal and stable after April 22. According to the data provided by the national center for space science, Chinese academy of sciences, the geomagnetic disturbance coefficient Kp and Dst index are at lower levels, which confirms ionospheric disturbance during this earthquake is not caused by geomagnetic storm or similar physical environment.

To further illustrate the ionospheric VTEC abnormalities during this earthquake, we check the results of two CMONOC stations near the epicenter, namely SCDF (30.978°N,101.122°E) and YNDC (26.108°N, 103.181°E). The real-time VTEC and VTEC quartiles time series are shown in Fig. 34.4. We observe that VTECs are below the lower bounds (L2) during the same period as for the epicenter.
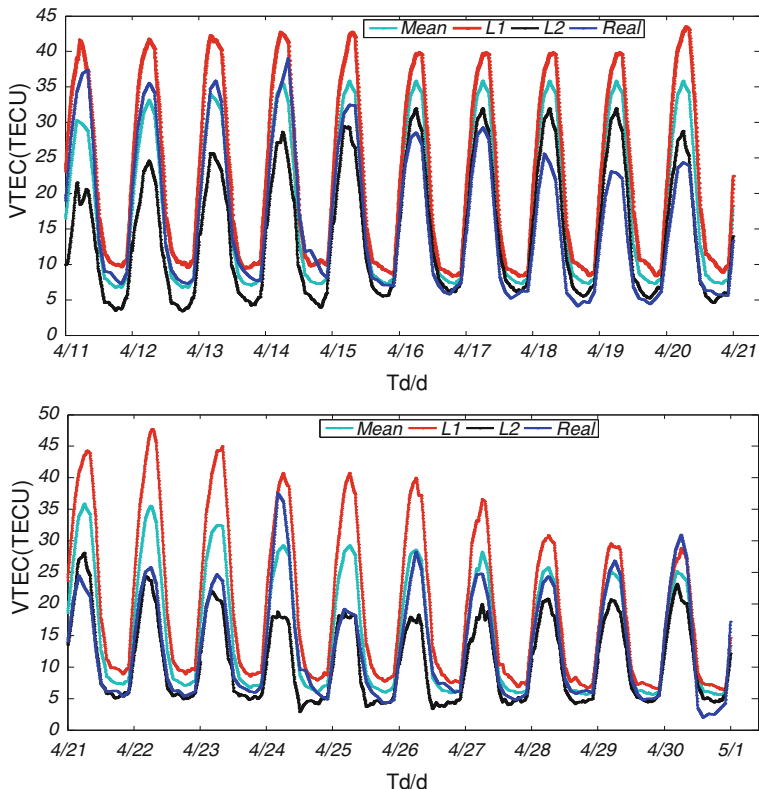
Fig. 34.3 Time series of VTEC over the epicenter of Lushan earthquake, where "mean" refers to the VTEC median over the same epoch of successive 15 days and "real" refers to real-time VTEC observed at each epoch

34.4 Coseismic Monitoring Using the CMONOC Network

With the fast development of high frequency GNSS technology, GNSS data plays an important role in instantaneous station motion monitoring and earthquake source rupture processing. Traditional GNSS high-frequency data processing is based on the Precise Point Positioning (PPP) or double difference baseline solution to obtain the instantaneous site displacements. However, the station position estimates are affected by unknown error resources and are limited by the capability of ambiguity fixing. Thus these strategies are still challenging for earthquake monitoring [12]. To overcome the limitations of the position solutions, the strategy of so-called instantaneous site velocity solution [13] is developed by using the GNSS Doppler observations.
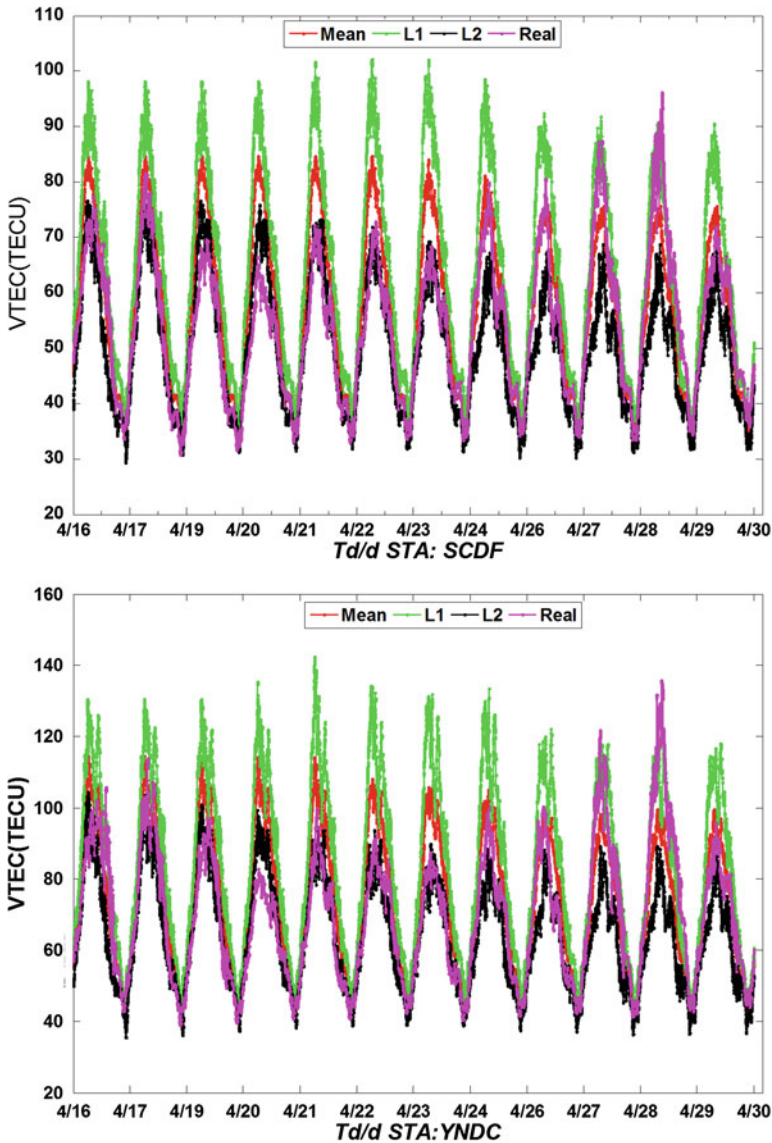
Fig. 34.4 Time series of VTEC for 4 stations during the Lushan earthquake, where "mean" refers to the VTEC median over the same epoch of successive 15 days and "real" refers to real-time VTEC observed at each epoch

Applying this strategy, we set up the coseismic monitoring system for the continuous station in the CMONOC network and the system runs in the following way: (1) retrieval of real-time high rate streams or files from internet protocols; (2)
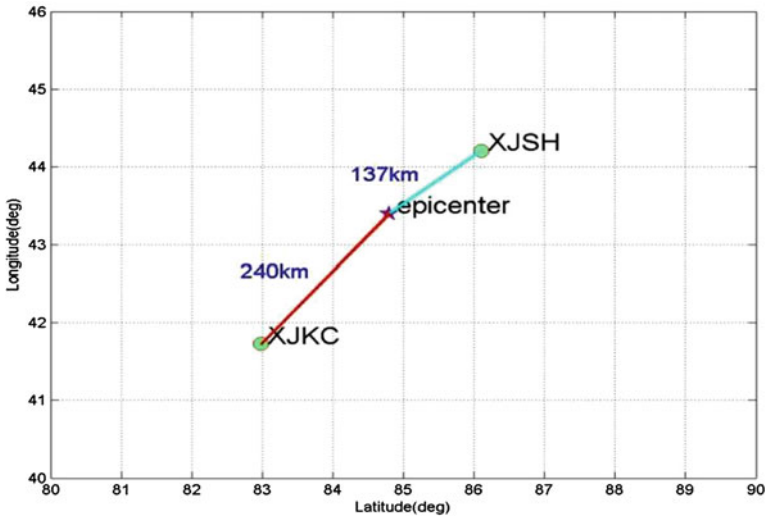
Fig. 34.5 Plot of the epicenter and selected stations

calculation of the Doppler observations from the phase observations, and esti-
mation of station instantaneous velocity based on Doppler observation; (3) check
for coseismic offsets based on the instantaneous solution.

Taking the Xinjiang Ms6.6 earthquake on June 30, 2012 as an example. The
earthquake happened at 05:07:31 (UTC 21:07:31 on June 29), and the stations
XJSH (137 km away from epicenter, sampling 1 s) and XJKC (240 km away from
epicenter, sampling 1 s) tracks the coseismic displacement. Figure 34.5 illustrates
the location of the epicenter and two stations. Using the above mentioned strategy,
we analysis the instantaneous velocity and coseismic offsets as shown in Figs. 34.6
and 34.7. The east components of the station velocity exhibit pure white noise
feature before the earthquake. The estimated instantaneous velocity and coseismic
offsets show obvious changes when the seismic waves reach these stations, where
maximum amplitude of instantaneous velocity reaches 16 mm/s for XJSH and
13 mm/s for XJKC, and the maximum coseismic offset reaches 11 mm for XJSH
and 10 mm XJKC, respectively. The shaking effects continue for around 20 s, the
stations become static and the estimated instantaneous velocity restore to white
noise after that. We observe that the epoch that seismic wave arrives at the station
XJSH is around 31 s ahead of the time it reaches XJKC. Based on the time
difference, we calculate the seismic waves speed as 3.32 km/s.

The high rate data of the CMONOC network is current archived in file with
latency of one day, and the coseismic monitoring is currently performed in post-
processing mode. With the stations being upgraded to real-time capability, the
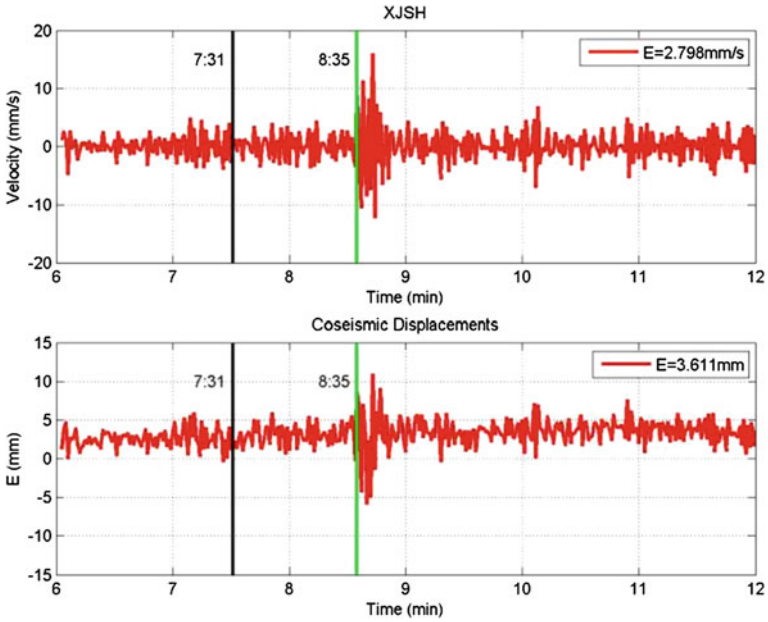system will support real-time coseismic monitoring.

Fig. 34.6 Velocity and coseismic displacement time series of station XJSH, 150 km away from epicenter
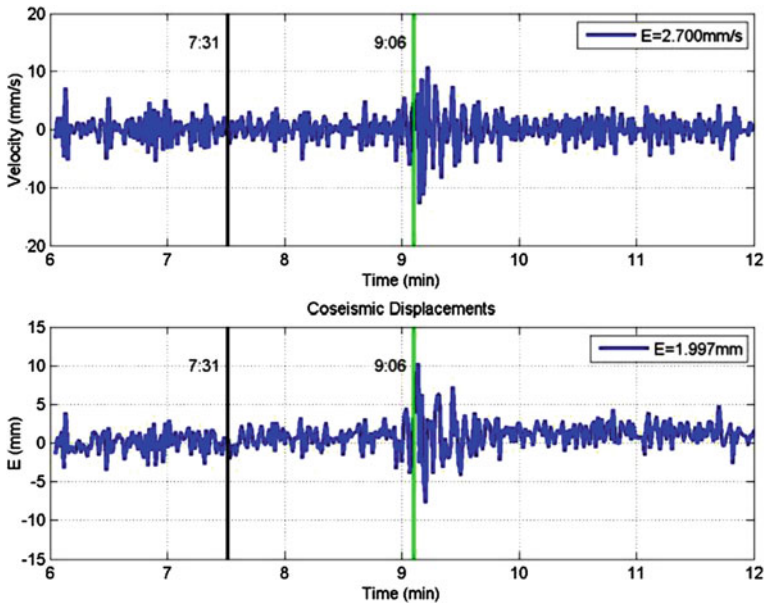

Fig. 34.7 Velocity and coseismic displacement time series of station XJKC, 250 km away from epicenter

34.5 Conclusion

We present the latest results from the CMONOC data analysis center at the SHAO. On the basis of the routine GNSS data analysis of the CMONOC and IGS sites, we present three new achievements: (1) the velocity field of continuous stations, which is released for the first time based on the combination of 3 years' daily solutions; (2) quartile based VTEC monitoring system, which is applied to the ionospheric disturbance monitoring during the Lushan earthquake; and (3) the instantaneous velocity strategy based coseismic monitoring system, with which the instantaneous velocity changes and coseismic offsets are monitored during the 2012 Xinjiang earthquake. The application of CMONOC data in earthquake monitoring could be realized in real-time with the network upgraded to real-time.

References

1. Wang Y, Liu L, Liang H, Ding K et al (2006) Research on precipitable water vapor in plateau and plain areas with GPS technique. J Geodesy Geodyn 26(1):88–92 (in Chinese)
2. Liu J, Shi C, Xu C, Jiang W (2001) Present day crustal movement speed field of China continent block using local repeated GPS network. Geomatics Inf Sci 26(3):189–195 (Journal of Wuhan University, in Chinese)
3. Junping C, Bin W, Xiaogong H, Haojun L (2012) Shanghai astronomical observatory CMONOC data analysis center. In: The 3rd China satellite navigation academic conference electronic proceedings-S08 satellite navigation model and method (in Chinese)
4. Junping C, Bin W, Xiaogong H, Haojun L (2012) SHA: the GNSS analysis center at SHAO. In: Proceedings of the 3rd China Satellite Navigation Conference, CSNC 2012, revised selected papers. Lecture Notes in Electrical Engineering, vol 160 LNEE, pp 213–221
5. Shanghai Observatory GNSS Analysis Center. http://www.shao.ac.cn/shao_gnss_ac
6. Dong D, Herring TA, King RW (1998) Estimating regional deformation from a combination of space and terrestrial geodetic data. J Geodyn 72:200–214
7. Danan D, Peng F et al (2006) Spatiotemporal filtering using principal component analysis and Karhunen-Loeve expansion approaches for regional GPS network analysis. J Geophys Res, 111:B03405
8. Min W, Zhengkang S, Zhijun N et al (2003) The crustal movement of and activity block model. Sci China 33:21–32 (in Chinese)
9. Ye S, Huang C (2000) Astrogeodynamics. Shandong Science and Technology Press, Shandong (in Chinese)
10. Barnes RA, Leonard RS (1965) Observations of ionospheric disturbance following the Alaska earthquake. J Geophys Res 70(9):1250–1253

11. Zhao Y, Zhang X, Liu J (2010) The ionospheric electron content disturbance analysis before and after the WenChun earthquake. Prog Geophys 25(4):447–453 (in Chinese)
12. Zhang X, Guo B (2013) Real-time tracking the instantaneous movement of crust during earthquake with a stand-alone GPS receiver. Chin J Geophys 56(2):1928–1936 (in Chinese)
13. Colosimo G, Crespi M, Mazzoni A (2011) Real-time GPS seismology with a stand-alone receiver: a preliminary feasibility demonstration. J Geophys Res 116:B11302. doi:10.1029/2010JB0079